eISSN 2005-5447
International Journal of Stem Cells Vol. 14, No. 2, 2021 https://doi.org/10.15283/ijsc20175

ORIGINAL ARTICLE

Enhancement of Wound Healing by Conditioned Medium of Adipose-Derived Stromal Cell with Photobiomodulation in Skin Wound

In-Su Park

Cell Therapy Center, Ajou University School of Medicine, Suwon, Korea

Background and Objectives: The objective of this study was to investigate whether conditioned medium from photobiomodulation (PBM) irradiated adipose-derived stromal cell (ASC) spheroids prior to implanting could stimulate angiogenesis and tissue regeneration to improve functional recovery of skin tissue in an animal skin wound model.
Methods and Results: ASC were split and seeded on chitosan-coated 24 well plate at a density of 7.5×10^4 cells/cm^2, and allowed to adhere at 37℃. Within 3 days of culture, ASC formed spheroids by PBM irradiation. Conditioned medium (CM) fractions were collected from the PBM-ASC to yield nor adipose-derived stromal cell spheroid (spheroid) and PBM-spheroid, respectively, centrifuged at 13,000 g at 4℃ for 10 min, and stored prior to use for ELISA, protein assay, or *in vivo* wound-healing assays. Phosphate-buffered saline, cultured CM from ASCs, PBM irradiation prior to implanting conditioned medium from ASC, cultured CM from ASC spheroid, and PBM–spheroid-CM (PSC) were transplanted into a wound bed in athymic mice to evaluate therapeutic effects of PSC *in vivo*. PSC enhanced wound closure in a skin injury model compared to PBS, CM, PBM–CM, and spheroid-CM. The density of vascular formations increased as a result of angiogenic factors released by the wound bed and enhanced tissue regeneration at the lesion site.
Conclusions: These results indicate that implant of PSC can significantly improve functional recovery compared to PBS, CM, PBM–CM, or spheroid-CM treatment. Implant of PSC may be an effective form of paracrine mediated therapy for treating a wound bed.

Keywords: Adipose-derived stromal cell, Spheroid, Angiogenesis, Photobiomodulation, Conditioned medium, Wound healing

Introduction

Reconstruction and replacement of skin loss, atrophy, and injury often need a certain amount of skin graft substitutes (1). On the other hand, the use of growth factors that can regulate cellular chemoattraction, proliferation, and differentiation has begun to be recognized as a new method for skin regeneration (2). Recent studies have confirmed that several growth factors such as bone morphogenetic proteins (BMPs), insulin-like growth factor (IGF)-1 and -2, transforming growth factor (TGF)-β1, platelet-derived growth factor (PDGF), and fibroblast growth factor (FGF)-2 could improve cellular ability to undergo wound healing by stimulating cellular events (3, 4).

Received: October 22, 2020, Revised: December 24, 2020, Accepted: December 31, 2020, Published online: February 28, 2021
Correspondence to **In-Su Park**
Cell Therapy Center, Ajou University School of Medicine, 403, San 5, Wonchon-dong, Youngtong-gu, Suwon 16499, Korea
Tel: +82-31-219-4440, Fax: +82-31-219-4442
E-mail: plaa91@naver.com

This is an open-access article distributed under the terms of the Creative Commons Attribution Non-Commercial License (http://creativecommons.org/licenses/by-nc/4.0/), which permits unrestricted non-commercial use, distribution, and reproduction in any medium, provided the original work is properly cited.

Copyright ⓒ 2021 by the Korean Society for Stem Cell Research

In particular, adipose-derived stem cells (ASCs) found in adipose tissue provide an attractive source of cell therapy for regeneration of damaged skin because they can self-renew and differentiate into various cells (5). However, this procedure suffers from some problems such as high financial investment due to expensive cell culture and complicated safety and quality management issues regarding cell handling. Like other cells utilized for cell-based therapy, ASCs may function through complex interactions with endogenous host cells and tissues via multiple mechanisms of action. ASCs can activate signal transduction pathways in target cells to encourage tissue regeneration (paracrine signaling theory) (6). However, only a small percentage of transplanted cells can integrate and survive in host tissues (7).

It has been reported that paracrine effects of growth factors and cytokines secreted from implanted ASCs may promote vascularization, tissue repair, and regeneration (8). A proper vascularization is very important to supply nutrients and oxygen to wound area in order to optimize wound healing (9). Angiogenesis is initiated by FGF, vascular endothelial growth factor (VEGF), and angiogenin. VEGF is a major mediator of angiogenesis to stimulate migration and proliferation of endothelial cells (10). Epithelialization is a regeneration of epidermis that is stimulated by epidermal growth factor (EGF), FGF-2, and hepatocyte growth factor (HGF) (11). Migration of epithelial cells will close the wound followed by proliferation and differentiation of epithelial cells to form epidermis layer (12, 13). Since cells within a spheroid are naturally exposed to mild hypoxia, they show enhanced cell viability and paracrine effects (14). Hypoxia can stimulate the production of growth factors such as VEGF, FGF, and HGF (15). Conditioned medium containing cytokine now can serve as a new treatment modality in regenerative medicine, showing successful outcome in some diseases (16). With the emergence of this approach, I have described the possibility of using stem cells conditioned medium as a novel and promising alternative to skin wound healing treatment (17). The application of stem cell culture derived conditioned medium as a therapy has been studied both *in vitro* and *in vivo* with excellent results (18). Therapy using conditioned medium is more promising than using stem cell itself due to the ease of production, packaging, and distribution. Conditioned medium fractions collected from photobiomodulation (PBM) cells have also been assessed for their contents of potentially beneficial cytokines, growth factors, and chemokines, and applied to cutaneous wounds in mice. PBM has positive biostimulatory effects on stem cells (19). For example, PBM can positively affect ASC by increasing cellular viability, proliferation, and migration (20, 21). PBM can also enhance secretion of VEGF, FGF, and HGF (19).

Paracrine factors secreted by ASC can accumulate in the conditioned media during cell culture. Conditioned media (CM) of ASC culture can serve multiple positive functions in tissue regeneration. CM may induce not only stem cell homing or mobilization into the injured tissues, but also trans-differentiation into several lineages of mesenchymal tissue. If these characteristics of CM can be exploited for skin regenerative medicine, CM may provide a substitute for ex vivo culture and implantation of ASC.

Thus, the objective of this study was to investigate whether photobiomodulation irradiation of conditioned medium from adipose-derived stromal cell spheroids (spheroid) prior to implanting could stimulate angiogenesis and tissue regeneration to improve functional recovery of skin tissue in an animal skin wound model.

Materials and Methods

Culture of ASCs

The ASC were supplied by Cell Engineering for Origin, CEFO (Seoul, Korea) under a material transfer agreement. ASC were isolated from the human- adipose tissue and were cultured in low-glucose Dulbecco's modified Eagle's medium F-12 (DMEM/F-12; Welgene, Daegu, Korea) supplemented with 10% fetal bovine serum (FBS, Welgene), 100 units/ml penicillin, and 100 μg/ml streptomycin at 37℃ in a 5% CO_2 incubator. The ASC between passage 5 and 8 were used for all experiments (Supplementary Fig. S1). ASC were stained with CD29, CD90 and CD105 for mesenchymal stem cell identification, with KDR, CD31 and CD34 for endothelial lineage cell identification (Supplementary Fig. S1).

Spheroid formation by photobiomodulation irradiation

ASC were split and seeded on chitosan-coated 24 well plate at a density of 7.5×10^4 cells/cm^2, and allowed to adhere at 37℃. Within 3 days of culture, ASC formed spheroids by photobiomodulation irradiation (L-spheroids). The light source used was LED (light emitting diode; WON Technology Co., Ltd., korea) designed to fit over a standard multi-well plate (12.5×8.5 cm) for cell culture. The LED was an emission wavelength peaked at 660 nm. The irradiance at the surface of the cell monolayer was measured by a power meter (Orion, Ophir Optronics Ltd., UT). To obtain the energy dose of 0～12 J/cm^2, exposure time for LED array was 10 min under power density of 0～20 mW/cm^2 (1 milliwatt×second=0.001 joules) (Su-

pplementary Table S1). L-spheroid sizes were measured by counting the area of individual cell clusters by image analysis. The diameters of spheroids were presented as median±SD (n=8 per group).

Preparation of conditioned medium

ASC were cultured under normoxic conditions in serum-containing complete medium for 24 h. The medium was then changed to serum-free a-MEM, and the cells were cultured under PBM conditions for another 48 h. Next, conditioned medium fractions were collected from the PBM-ASC to yield nor spheroid and PBM- spheroid, respectively, centrifuged at 13,000 g at 4℃ for 10 min, and stored prior to use for enzyme linked immune sorbent assays (ELISAs), *in vitro* cell proliferation and migration assays, or *in vivo* wound-healing assays. For the *in vivo* wound-healing analysis, aliquots of conditioned media were concentrated by further centrifugation and filtration through a centrifugal filter unit (Millipore, Billerica, MA, USA). Protein of CM was quantified using the BCA assay, equal quantities of protein were experimented.

Human angiogenic protein analysis

To analyze the expression profiles of angiogenesis-related proteins, I used a Human Angiogenesis Array Kit (R&D Systems, Ltd., Abingdon, UK). Cell samples (5×10^6 cells) were harvested, and 150 μg of protein were mixed with 15 μl of biotinylated detection antibodies. After pre-treatment, the cocktail was incubated with the array overnight at 4℃ on a rocking platform. Following washing to remove unbound material, streptavidin–horseradish and chemiluminescent detection reagents are added sequentially. The signals on the membrane film were detected by scanning on an image reader LAS-3000 (Kodak, Rochester, NY) and were quantified using the MultiGauge 4.0 software (Kodak). The positive signals seen on developed film were identified by placing a transparency overlay on the array image and aligning it with the two pairs of positive control spots in the corners of each array.

ELISA assay for angiogenic growth factor production

Angiogenic growth factor production in the spheroid was assayed with a commercially available ELISA kit (R&D Systems) according to the manufacturer's protocols. The concentrations are expressed as the amount of angiogenic growth factor per 10^4 cells at a given time.

Immunofluorescence staining

Indirect immunofluorescence staining was performed using a standard procedure. In brief, tissues cryosectioned at a 4-μm thickness were fixed with 4% paraformaldehyde, blocked with 5% BSA/PBS (1 h, 24℃), washed twice with PBS, treated with 0.1% Triton X-100/PBS for 1 min, and washed extensively in PBS. The sections were stained with specific primary antibodies and fluorescent-conjugated secondary antibodies (Supplementary Table S2) using a M.O.M kit according to the manufacturer's instructions (Vector Laboratories, Burlingame, CA). The cells were counterstained with DAPI (4,6-diamino-2-phenylindole dihydrochloride; Vector Laboratories). Mouse IgG (Dako, Carpinteria, CA) and rabbit IgG (Dako) antibodies was used as negative controls. To detect transplanted human cells, sections were immunofluorescently stained with anti-human nuclear antigen (HNA, Millipore). The stained sections were viewed with a DXM1200F fluorescence microscope (Nikon, Tokyo, Japan). The processed images were analyzed for fluorescence intensity using the ImageJ software (NIH).

Histological staining

Samples were harvested 14 days after treatment. Specimens were fixed in 10% (v/v) buffered formaldehyde, dehydrated in a graded ethanol series, and embedded in paraffin. Specimens were sliced into 4 μm-thick sections and were stained with hematoxylin and eosin (H&E) to examine muscle degeneration and tissue inflammation. Masson's trichrome collagen staining was performed to assess tissue fibrosisin ischemic regions. The criteria used for the histological scores of wound healing were summarized in Supplementary Table S3. The histological parameters considered were reepithelialization, dermal regeneration, granulation tissue formation, and angiogenesis (15). Regeneration of skin appendages was assessed by counting the number of hair follicles or sebaceous glands in the wound bed.

Western blot analysis

Samples were solubilized in lysis buffer [20 mM Tris-HCl, pH 7.4, 150 mM NaCl, 1 mM EDTA, 1% Triton X-100, 0.1% sodium dodecyl sulfate (SDS), 1 mM phenylmethylsulfonyl fluoride, 1 μg/ml leupeptin, and 2 μg/ml aprotinin] for 1 h at 4℃. The lysates were then clarified by centrifugation at 15,000 g for 30 min at 4℃, were diluted in Laemmli sample buffer containing 2% SDS and 5% (v/v) 2-mercaptoethanol, and were heated for 5 min at 90℃. The proteins were separated via SDS polyacrylamide gel electrophoresis (PAGE) using 10% or 15% resolving gels followed by transfer to nitrocellulose membranes (Bio-Rad, Hercules, CA) and then probed with antibodies against HIF-1a (Novus), CD31 (Abcam), HGF

(Santa cruz), VEGF (Abcam), and FGF2 (Abcam) for 1 h at room temperature (Supplementary Table S2). Peroxidase-conjugated anti-mouse IgG or anti-rabbit IgG and enhanced chemiluminescence (Amersham Pharmacia Biotech, Piscataway, NJ) were used as described by the manufacturer for detection. The membranes were scanned to create chemiluminescent images that were then quantified with an image analyzer (Kodak).

Preparation of the experimental animal model

The animal studies were approved by the Dankook University Animal Use and Care Committee. Five-week-old male BALB/c nude mice (20 g body weight; Narabio, Seoul, Korea) were anesthetized with ketamine (100 mg/kg). After aseptically preparing the surgical site, two full-thickness skin wounds were created on the dorsal part using an 8-mm biopsy punch. To inhibit wound contraction, a 0.5-mm thickness silicone splint was applied, as has been

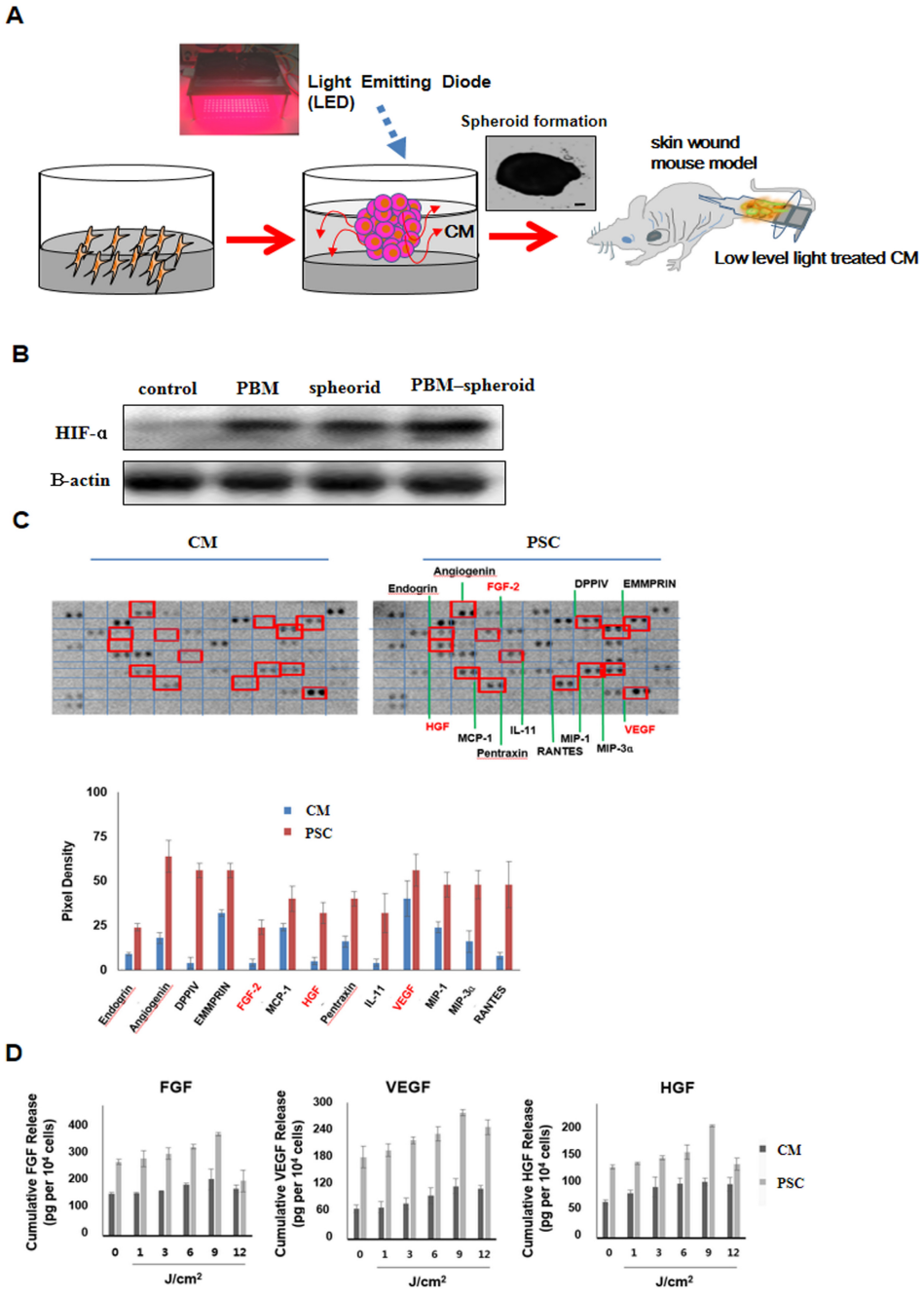

Fig. 1. ASC formed spheroids by Low-Level light irradiation. (A) Brief overview of our experiment procedure. The light source used was LED (660 nm) designed to fit over a microplate (12.5×8.5 cm) for spheroid formation. ASC morphology on 24 well polystyrene plate at 72 h. Scale bar=500 μm. (B) Western blot analysis and quantification of hypoxia-induced survival factor as hypoxia-inducible factor (HIF)-1 α in ASC cultured as spheroids, PBM.AS, and monolayers. (C) Enhanced secretion of angiogenic growth factors from PBM.AS in the wound bed. Angiogenesis-related protein analysis of PBM.AS (*, $p<0.05$, compared to the CM group, t-test, n=3 in each group). (D) ELISA measurement of spheroids cultured for 3 days. Concentrations of VEGF are presented as pg-corrected for 10^4 cells (*, $p<0.05$, compared with spheroid 6 J/cm^2 group, t-test, n=3 in each group).

previously described (22). The splint was fixed with instant adhesive and six simple, interrupted sutures around the wound with Nylon 6-0. The wounds were randomly classified into five groups: (1) Phosphate-Buffered Saline (PBS group, n=9), (2) conditioned medium from adipose-derived stromal cell (CM group, n=9), (3) conditioned medium from photobiomodulation irradiated adipose-derived stromal cell (PBM–CM group, n=9), (4) conditioned media from adipose-derived stromal cell spheroid (spheroid-CM group, n=9), and (5) conditioned medium from photobiomodulation irradiated adipose-derived stromal cell spheroids (PSC group, n=9). Each mouse received an injection of 0.8 ml of the CM per day for three consecutive days. CM were implanted intradermally at four injection sites on the border between the wound and the normal skin. The control group received an injection of PBS. During the treatment period, behavioral changes were observed and recorded, and the effect of treatment on survival was recorded. The physiological status of the wound was followed up for up to 2 weeks after treatment. Tegaderm (3M Health Care, MN, USA) was used for wound protection, and an equivalent volume of CM were injected in both conditions.

Gross evaluation of the wound area

The wounds were photographed using a digital camera at 3, 7, and 14 days after surgery, and the wound area was measured by tracing the wound margin and then performing the calculation using the Image J image analysis program (NIH, MD, USA). The wound area was analyzed by calculating the percentage of the current wound with respect to the original wound area. The wound was considered to be completely closed when the wound area was grossly equal to zero.

Statistical analyses

All quantitative results were obtained from triplicate samples. Data were expressed as a mean±SD, and the statistical analyses were carried out using two-sample t tests to compared two groups of samples and a One-way Analysis of Variance (ANOVA) for the three groups. A value of $p<0.05$ was considered to be statistically significant.

Results

Production of angiogenic factors

ASCs were cultured on non-tissue culture-treated 24-well plates in the presence of fital bovine serum (FBS) and formed a floating spheroid after irradiation with PBM (Fig. 1A) at 3 days after seeding. Diameters of most spheroids ranged from 1.2 to 1.5 mm. Spheroid cultures showed significant increase in expression of hypoxia-induced survival factors such as hypoxia-inducible factor (HIF)-1α, relative to cells in a monolayer culture (Fig. 1B). HIF-1α is known to upregulate the expression of angiogenic growth factors (23, 24). L-spheroid ASCs showed considerable expression of angiogenic growth factors, *i.e.*, hepatocyte growth factor (HGF), vascular endothelial growth factor (VEGF), and fibroblast growth factor 2 (FGF2) (Fig. 1C). The expression of angiogenic growth factors in PBM-spheroid (energy dose of 9 J/cm^2) was much greater than that in ASCs cultured in a monolayer culture (Fig. 1D).

Enhanced secretion of growth factors from implanted CM in wound bed

Immunofluorescent staining of angiogenic growth factors bFGF, VEGF, and HGF indicated the presence from implanted CM (Fig. 2A). More growth factor were observed in the PSC implanted group compared to CM group. Western blot assay showed significantly higher levels of VEGF, bFGF, and HGF in PSC implanted group than those in the CM (control group). Greater amounts of growth factors were also observed in the PSC group than those in the CM group (Fig. 2B). However, no significant difference was observed in expression of growth factors between CM or PSC treated tissues and spheroid-CM treated tissues.

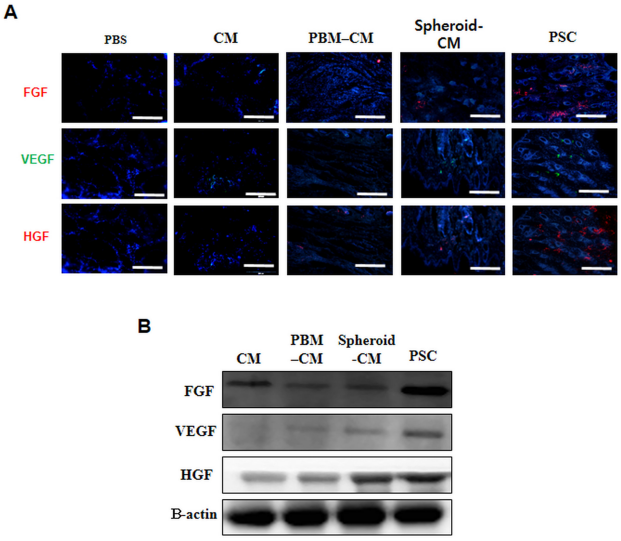

Fig. 2. Enhanced secretion of angiogenic growth factors in the wound bed. (A) Immunostaining was performed with anti-bFGF and anti-VEGF or anti-HGF antibody (red) at 14 days. The scale bar indicates 100 μm. (B) Western blot indicating the expression of bFGF, VEGF, and HGF at 14 days.

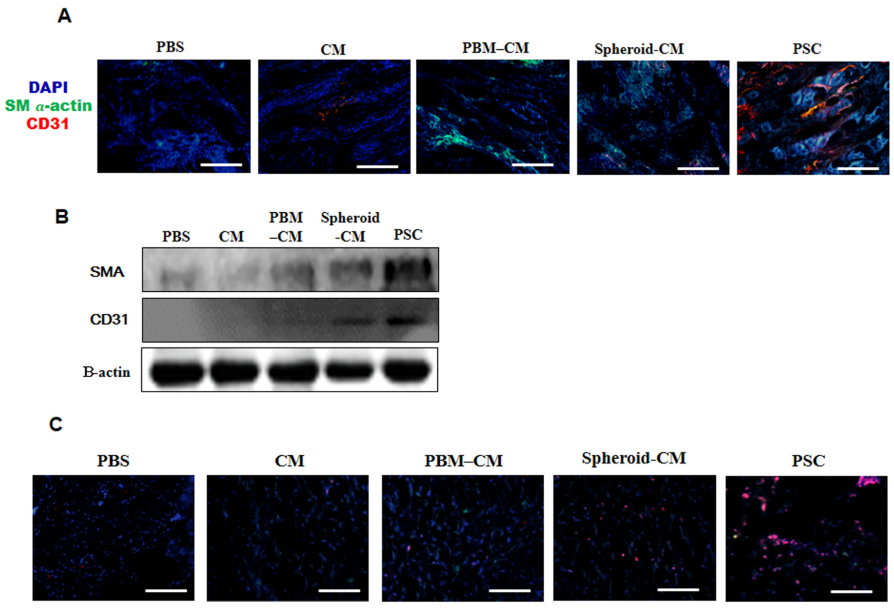

Fig. 3. Angiogenic efficacy in the wound bed. (A) Implants were removed on day 14 after implanted and stained with anti CD31 and α SMA antibodies. The scale bar indicates 200 μm. (B) Western blot showing the expression of CD31 and αSMA at 14 days. Beta-actin, also known as a "housekeeping" protein, is used as a loading control. (C) Immunofluorescence images showing cytokeratin-positive epithelial cells (red) at 14 days. The scale bar indicates 20 μm.

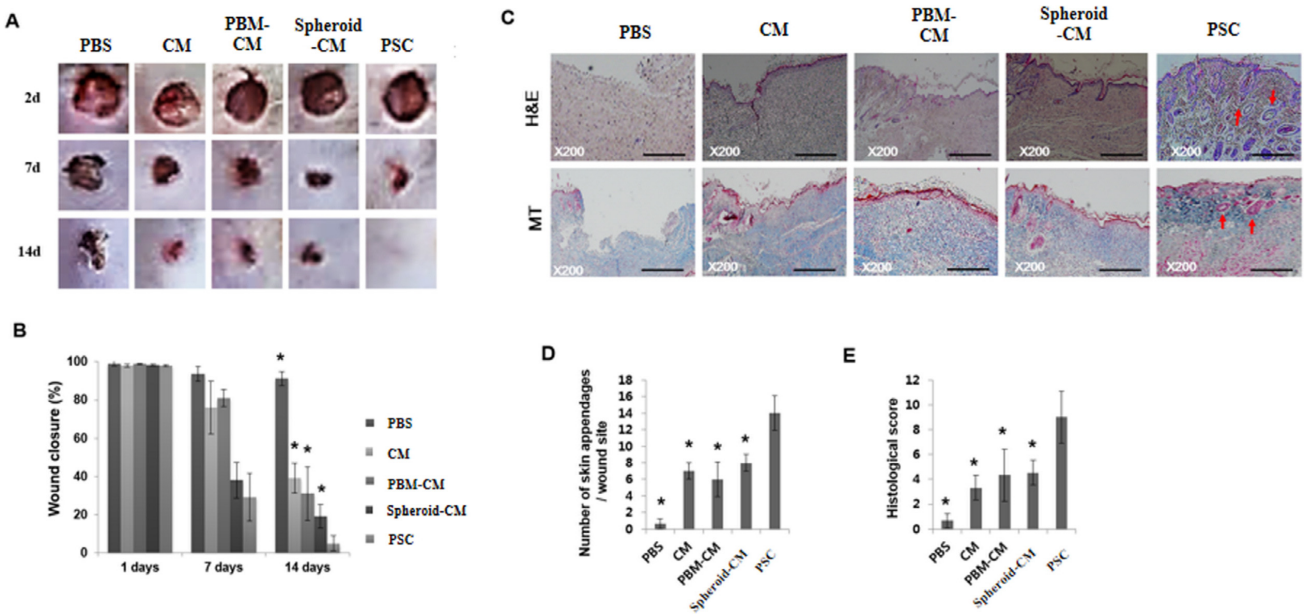

Fig. 4. Evaluation of wound closure. (A) The prepared excisional wound splinting model. Photographs of wounds. (B) Percentage of wound area was calculated using photographs of wounds at 1, 7, and 14 days. *$p<0.05$ versus the PSC group. (C) Histological analysis of the wound bed. Wounds were stained with H&E and Masson's trichrome at 14 days. Wound edges are indicated with arrowheads. Closed arrows indicate skin appendages (hair follicles). The scale bar indicates 500 μm. (D) Regeneration of skin appendages was investigated by counting the number of skin appendages per wound section. (E) Histological scoring was performed using the criteria presented in Supplementary Table S3. *$p<0.05$ versus the PSC group.

Angiogenic efficacy in the wound bed

Many CD31+ cells in the PSC group were double stained for smooth muscle actin (SMA). ECs and perivascular cells differentiated from injected human cells were detected via αSMA and CD31 antibodies, respectively (Fig. 3A). Western blot assay revealed significantly higher levels of CD31 secreted by spheroid and PSC groups than those by the control group. Western blot also showed greater amounts of growth factors in the PSC group than those in the ASC group (Fig. 3B). However,

there was no significant difference in levels of growth factors among PBS, CM, PBM–CM, and spheroid-CM. These findings suggest a greater effectiveness of PSC treatment for angiogenesis in the wound bed.

Epithelial cells

To determine whether PSC could contribute to the epidermal structure, immunohistochemistry for pan-cytokeratin was performed at 14 days. Some cytokeratin-positive cells were found in the epidermis or sebaceous glands in the PSC (Fig. 3C).

Wound closure and dermal reaction

An excisional wound splinting model was prepared. Silicon splints remained tightly adherent to the skin and restricted wound contraction during the experimental period (Fig. 4A). At 7 days after surgery, the PSC group exhibited significantly smaller wound areas than other groups. At 7 days, the PSC group showed a significantly smaller wound area than PBS, CM, PBM–CM, or spheroid-CM group. No significant difference in wound area was observed between PBS group at any time (Fig. 4B). At 14 days, all wounds of the PSC group achieved complete closure. However, not all wounds of the PBS, CM, PBM–CM, or spheroid-CM group had completely closed. Histological observation showed that skin regeneration was much greater in the PSC group compared to the control group. Our data indicated that the PSC enhanced re-epithelialization and granulation at 14 days (Fig. 4C). Furthermore, the PSC group appeared to have an increased number of skin appendages (Fig. 4D). The PSC group displayed significantly increased numbers of hair follicles and sebaceous glands at 14 days (Fig. 4E).

Discussion

Cutaneous wound healing encompasses a highly complex process involving an orderly regulated cascade of events, including cells migration and proliferation, extracellular matrix (ECM) deposition, angiogenesis, and remodeling (25). Optimal wound healing requires a well-orchestrated integration of numerous molecular and cellular events that are mediated by growth factors, cytokines, and chemokines. FGF, HGF, and VEGF are among growth factors and cytokines known to enhance normal wound healing (4).

The formation of spheroids is affected by the cell-matrix adhesion strength (26). Moreover, PBM can promote the migration of ASC (27). In this study, within 3 days of culture on 24-well plates, ASC formed spheroids as a result of PBM irradiation (Fig. 1A). Notably, an increased HIF-1 α expression and consequent induction of VEGF and FGF proteins occurred at a fluence of 660 nm (8, 28). It has been previously reported that hypoxia can mediate angiogenic switch in agglomerates of tumor cells larger than 200 μm in diameter (29). In our experimental model, I observed that the non-irradiated group expressed HIF-1α in response to the hypoxic environment formed in the hASC spheroid. In the irradiated group, 660-nm light alone was able to increase HIF-1α expression in this model regardless of fluence used. Therefore, ASCs in the spheroid might have been up-regulated by angiogenic factors such as VEGF (Fig. 2D).

In this study, PSC accelerated wound closure with increased levels of re-epithelialization, neovascularization, and regeneration of skin appendages. This is likely to be due to increased paracrine secretion (Fig. 2). These results indicate that PSC has the ability to promote regeneration of skin tissue. Thus, PSC may be more feasible and practical to use in wound healing than ASC themselves. It is possible that PBM can enhance cellular responses in terms of gene expression, secretion of growth factors, and cell proliferation by increasing mitochondrial membrane potential and levels of ATP and cAMP (28). VEGF is the most effective and specific growth factor that regulates angiogenesis (3); bFGF is an important growth factor in wound healing because it affects migration and proliferation of fibroblasts, angiogenesis, and matrix deposition (4). HGF is another potent proangiogenic factor that can induce migration and proliferation and inhibit apoptotic cell death (30).

PSC appeared to promote vasculogenesis through a synergistic effect in the wound bed, indicating that the PSC was more effective than CM in increasing angiogenic growth factor expression (Fig. 3A). Recent cell therapy for regeneration of damaged skin aims to increase vascularization to a sufficient level for wound perfusion and healing (31). Formation of new blood vessels is critical for normal wound healing. Angiogenesis aids in the repair of damaged tissue by regenerating blood vessels, thus improving blood flow in skin wounds (1). In addition to sebaceous glands, some cytokeratin positive cells were observed in the regenerated epidermis (Fig. 3C). In this study, the PSC group exhibited rapid wound closure and a higher histological score relative to the spheroid-CM group (Fig. 4). In skin bioengineering, the ultimate goal is to rapidly produce a construct that offers complete restoration of functional skin, ideally involving regeneration of all skin appendages and layers (2). Interestingly, our results showed that the PSC group presented significantly in-

creased numbers of sebaceous glands than the spheroid-CM group. PSC implanted accelerated tissue regeneration through the growth factor secretion. For that reason, I emphasize the significance of the application of a 3D spheroid culture of stem cells with PBM to enhance treatment efficiency of PSC implanted relative to CM implanted in the wound bed.

Results of this study demonstrate considerable influence of PBM on biological properties of ASC, indicating an intriguing possibility that ASC-derived products might find utility in cell-free therapies to encourage healing of intractable skin wounds.

Acknowledgments

This research was supported by the National Research Foundation (NRF) and ministry of SMEs and startups funded by the Korean government (NRF-2020R1I1A1A01058248, SMEs-S2957289).

Potential Conflict of Interest

The authors have no conflicting financial interest.

Supplementary Materials

Supplementary data including three tables and one figure can be found with this article online at https://doi.org/10.15283/ijsc20175

References

1. Kyriakides TR, Maclauchlan S. The role of thrombospondins in wound healing, ischemia, and the foreign body reaction. J Cell Commun Signal 2009;3:215-225
2. Metcalfe AD, Ferguson MW. Bioengineering skin using mechanisms of regeneration and repair. Biomaterials 2007;28:5100-5113
3. Nie C, Yang D, Morris SF. Local delivery of adipose-derived stem cells via acellular dermal matrix as a scaffold: a new promising strategy to accelerate wound healing. Med Hypotheses 2009;72:679-682
4. Heydarkhan-Hagvall S, Schenke-Layland K, Yang JQ, Heydarkhan S, Xu Y, Zuk PA, MacLellan WR, Beygui RE. Human adipose stem cells: a potential cell source for cardiovascular tissue engineering. Cells Tissues Organs 2008;187:263-274
5. Gimble J, Guilak F. Adipose-derived adult stem cells: isolation, characterization, and differentiation potential. Cytotherapy 2003;5:362-369
6. Joggerst SJ, Hatzopoulos AK. Stem cell therapy for cardiac repair: benefits and barriers. Expert Rev Mol Med 2009;11:e20
7. Don CW, Murry CE. Improving survival and efficacy of pluripotent stem cell-derived cardiac grafts. J Cell Mol Med 2013;17:1355-1362
8. Park IS, Chung PS, Ahn JC. Adipose-derived stem cell spheroid treated with low-level light irradiation accelerates spontaneous angiogenesis in mouse model of hindlimb ischemia. Cytotherapy 2017;19:1070-1078
9. Li P, Guo X. A review: therapeutic potential of adipose-derived stem cells in cutaneous wound healing and regeneration. Stem Cell Res Ther 2018;9:302
10. Valcárcel M, Arteta B, Jaureguibeitia A, Lopategi A, Martínez I, Mendoza L, Muruzabal FJ, Salado C, Vidal-Vanaclocha F. Three-dimensional growth as multicellular spheroid activates the proangiogenic phenotype of colorectal carcinoma cells via LFA-1-dependent VEGF: implications on hepatic micrometastasis. J Transl Med 2008;6:57
11. Pastar I, Stojadinovic O, Yin NC, Ramirez H, Nusbaum AG, Sawaya A, Patel SB, Khalid L, Isseroff RR, Tomic-Canic M. Epithelialization in wound healing: a comprehensive review. Adv Wound Care (New Rochelle) 2014;3:445-464
12. Wu Y, Chen L, Scott PG, Tredget EE. Mesenchymal stem cells enhance wound healing through differentiation and angiogenesis. Stem Cells 2007;25:2648-2659
13. Nie C, Yang D, Xu J, Si Z, Jin X, Zhang J. Locally administered adipose-derived stem cells accelerate wound healing through differentiation and vasculogenesis. Cell Transplant 2011;20:205-216
14. Park IS, Rhie JW, Kim SH. A novel three-dimensional adipose-derived stem cell cluster for vascular regeneration in ischemic tissue. Cytotherapy 2014;16:508-522
15. Park IS, Kim SH, Jung Y, Rhie JW, Kim SH. Endothelial differentiation and vasculogenesis induced by three-dimensional adipose-derived stem cells. Anat Rec (Hoboken) 2013;296:168-177
16. Pawitan JA. Prospect of stem cell conditioned medium in regenerative medicine. Biomed Res Int 2014;2014:965849
17. Kanji S, Das H. Advances of stem cell therapeutics in cutaneous wound healing and regeneration. Mediators Inflamm 2017;2017:5217967
18. Chen P, Chen JZ, Shao CY, Li CY, Zhang YD, Lu WJ, Fu Y, Gu P, Fan X. Treatment with retinoic acid and lens epithelial cell-conditioned medium in vitro directed the differentiation of pluripotent stem cells towards corneal endothelial cell-like cells. Exp Ther Med 2015;9:351-360
19. Choi K, Kang BJ, Kim H, Lee S, Bae S, Kweon OK, Kim WH. Low-level laser therapy promotes the osteogenic potential of adipose-derived mesenchymal stem cells seeded on an acellular dermal matrix. J Biomed Mater Res B Appl Biomater 2013;101:919-928
20. Mvula B, Mathope T, Moore T, Abrahamse H. The effect of low level laser irradiation on adult human adipose derived stem cells. Lasers Med Sci 2008;23:277-282
21. Mvula B, Moore TJ, Abrahamse H. Effect of low-level laser irradiation and epidermal growth factor on adult human adipose-derived stem cells. Lasers Med Sci 2010;25:33-39

22. Wang X, Ge J, Tredget EE, Wu Y. The mouse excisional wound splinting model, including applications for stem cell transplantation. Nat Protoc 2013;8:302-309
23. Kapur SK, Wang X, Shang H, Yun S, Li X, Feng G, Khurgel M, Katz AJ. Human adipose stem cells maintain proliferative, synthetic and multipotential properties when suspension cultured as self-assembling spheroids. Biofabrication 2012;4:025004
24. Glicklis R, Merchuk JC, Cohen S. Modeling mass transfer in hepatocyte spheroids via cell viability, spheroid size, and hepatocellular functions. Biotechnol Bioeng 2004;86:672-680
25. Chen M, Przyborowski M, Berthiaume F. Stem cells for skin tissue engineering and wound healing. Crit Rev Biomed Eng 2009;37:399-421
26. Santini MT, Rainaldi G, Indovina PL. Apoptosis, cell adhesion and the extracellular matrix in the three-dimensional growth of multicellular tumor spheroids. Crit Rev Oncol Hematol 2000;36:75-87
27. Ginani F, Soares DM, Barreto MP, Barboza CA. Effect of low-level laser therapy on mesenchymal stem cell proliferation: a systematic review. Lasers Med Sci 2015;30:2189-2194
28. Hu WP, Wang JJ, Yu CL, Lan CC, Chen GS, Yu HS. Helium-neon laser irradiation stimulates cell proliferation through photostimulatory effects in mitochondria. J Invest Dermatol 2007;127:2048-2057
29. Bhang SH, Cho SW, La WG, Lee TJ, Yang HS, Sun AY, Baek SH, Rhie JW, Kim BS. Angiogenesis in ischemic tissue produced by spheroid grafting of human adipose-derived stromal cells. Biomaterials 2011;32:2734-2747
30. Lee EJ, Park HW, Jeon HJ, Kim HS, Chang MS. Potentiated therapeutic angiogenesis by primed human mesenchymal stem cells in a mouse model of hindlimb ischemia. Regen Med 2013;8:283-293
31. Alev C, Ii M, Asahara T. Endothelial progenitor cells: a novel tool for the therapy of ischemic diseases. Antioxid Redox Signal 2011;15:949-965